



## Synthesis of high transparency of F doped NiO monocrystalline thin films by spray deposition

M Mammi<sup>1</sup>, S Benramache<sup>2</sup>, Y Aoun<sup>3</sup>, and A Sbaihi<sup>2</sup>

<sup>1</sup>Department of Physics, University of El-Oued, 39000, Algeria.

<sup>2</sup>Laboratoire des Matériaux, des Énergies et de l'Environnement, University of Biskra 07000, Algeria,

<sup>3</sup>Mechanical Department, Faculty of Technology, University of El-Oued, El-Oued 39000, Algeria

E-mail: s.benramache@univ-biskra.dz,

(Received 4 November 2023; in final form 9 December 2023)

### Abstract

The main objective of this work is to investigate a new material based on fluorine doped NiO thin films by spray deposition technique. Nickel nitrate hexahydrate  $\text{Ni}(\text{NO}_3)_2 \cdot 6\text{H}_2\text{O}$  and ammonium fluoride ( $\text{NH}_4\text{F}$ ) with a ratio of  $\text{F}/\text{Ni} = 0.04$  were used to prepare F doped NiO. The structural, optical and electrical properties of F doped NiO thin films were investigated with different NiO:F solution volumes of 5, 10, 15 and 20 ml using the spray technique. The prepared F doped NiO thin films have a monocrystalline nature with a cubic structure; the (111) diffraction peak is the preferred orientation; the maximum crystallite size is 19.21 nm obtained for 20 ml. The optical property shows that the all the prepared F doped NiO thin films have a good transmittance of about 80 % in the visible region. The F doped NiO thin films deposited with 20 ml have a minimum optical gap energy of 3.51 eV and the highest value of Urbach energy of 0,689 meV. However, the thin film prepared with 5 ml has a minimum electrical resistivity of 231  $\Omega \cdot \text{cm}$ , which can be used as a gas sensing.

**Keywords:** F, NiO, thin films, spray deposition technique, monocrystalline structure.

### 1. Introduction

Recent research shows that semiconductor metal oxides are essential compounds for the development of ultrahigh frequency devices, photocatalysis, optoelectronics, gas sensors, lithium ion microbatteries and cathode materials for alkaline batteries [1-3]. However, nickel oxide (NiO) is a direct large-gap (3.6-4.0 eV), semi-transparent p-type semiconductor material with a wide range of applications, represented by gas sensors, ultraviolet photo detectors, dye-sensitizers, photocatalysis, photovoltaic coatings, and lightweighting [1-6], the structural components in aerospace, in ceramic structures, counter electrodes and the anode layer of solid electrode oxide fuel cells [2-9]. On the other hand, nickel oxide has a cubic structure and NiO has a good transparency in the thin film [10-12].

NiO has recently focused on doping NiO with transition metals (TMs) such as Cu [2], Na [3], Zn [4], V [6], Mn [10], Al, Ga, In [12], Li [13], Ag [14], Mg [15], Co [16], and Mo [17] in cooperation with Ni to increase electrical conductivity. However, there is a new doping effect on optical properties; which is fluorine doped NiO thin films. The F doping can be used to increase the transmission and to increase the movement of F in the NiO:F.

The aim of this work is to study F doped NiO thin films with the help of organic solar cells for electrical energy harvesting. The organic solar cells consisted of an inner mirror layer inside (ITO glass) and a substrate holder. F doped NiO thin films can be deposited on a glass substrate by the spray pneumatic method with different volumes of 5, 10, 15 and 20 ml of the NiO:F mixture. The F doped NiO thin films were characterised by various methods, including X-ray diffraction, UV-vis spectrophotometry, and four-point techniques.

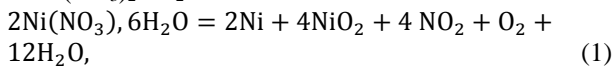
### 2. Experiments

The prepared solution of NiO was dissolved by 0.10  $\text{mol} \cdot \text{l}^{-1}$  of nickel nitrate hexahydrate  $\text{Ni}(\text{NO}_3)_2 \cdot 6\text{H}_2\text{O}$  (industrial powder with 99 purity) and ammonium fluoride ( $\text{NH}_4\text{F}$ ) (industrial powder with 97 purity) with the ratio of  $\text{F}/\text{Ni} = 0.04$ , the mixture powder was dissolved in the same volumes absolute of water  $\text{H}_2\text{O}$ , we have added drops of HCl solution for stabilisation.



**Figure 1.** A photograph of the experimental setup for the deposition of F-doped NiO thin films.

The mixture solution was stirred and heated at 45°C until a time of 4 h to transparent solution. F doped NiO thin films were sprayed onto the heated glass substrates at 450 °C with different solution volumes using the organic solar cells, and the volumetric spray rate was 0.1 ml/s. The structure of the spray deposition system and the fabricated organic solar cells are shown in figure 1. In this work, we used a digital display thermocouple (C100FK02 - M\*AN) to determine the temperature, which it determined between 400 and 600 °C. However, the direct calcinations of  $\text{Ni}(\text{NO}_3)_2 \cdot 6\text{H}_2\text{O}$  follows the reaction as:



The thin films of F doped NiO were characterised by different techniques to find the crystalline structure, optical transmission and electrical conductivity, which it are the respectively the X-ray diffraction (XRD Bruker AXS-8D with  $\lambda = 0.15406$  nm), spectrophotometer (UV-Lambda 35 with 300–900 nm of wavelength), and the four point techniques of the instrument Keithley Model 2400 Low Voltage Source Meter instrument.

### 3. Results and discussion

Figure 2 shows the crystal structure of F-doped NiO thin films prepared at different NiO:F solution volumes of 5, 10, 15 and 20 ml and NiO at 10 ml.

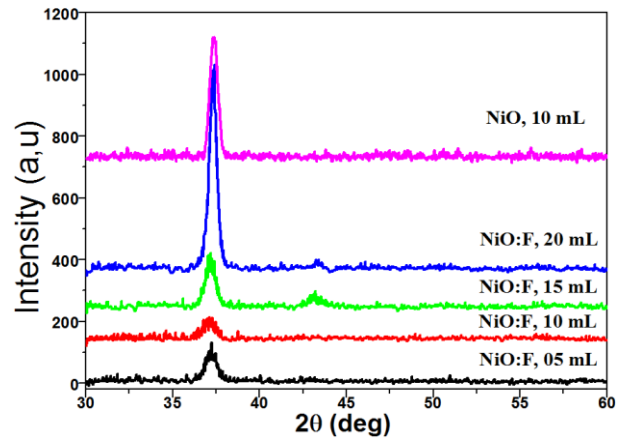


**Figure 2.** The results of X-ray diffraction spectra of undoped and F-doped NiO thin films at different NiO:F volumes.

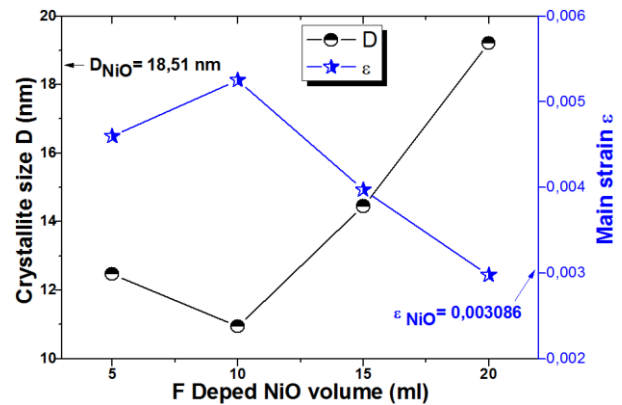


**Figure 3.** The results of crystallite size  $D$  (111) and main strain  $\varepsilon$  of F undoped and doped NiO thin films at different NiO:F volumes.

As a first result, we have found that all the films exhibited a diffraction peak at  $2\theta = 37$  related to the (111) plane of the NiO phase, which is a single crystal cubic structure. It can be seen that the thin film of F doped NiO deposited with 20 ml has a good crystal structure showed for a highest and strong peak, which confirm that the increase in the deposition volume can be improve the crystalline quality of F doped NiO thin films.

The crystal structure of F-doped NiO thin films represented by crystallite size  $D$  (111) and main strain  $\varepsilon$  was calculated using the following equations [16-18]:

$$D = \frac{0.9\lambda}{\beta \cos\theta}, \quad (2)$$

$$\varepsilon = \frac{\beta}{4 \tan\theta}, \quad (3)$$

where  $D$  is the crystallite size,  $\lambda$  is the X-ray wavelength ( $\lambda = 1.5406$  Å),  $\beta$  is the full width at half-maximum (FWHM), and  $\theta$  is the angle of diffraction peak and  $\varepsilon$  is the main strain.

Figure 3 shows the variation of the crystallite size and the main strain of F doped NiO thin films at different volumes. As can be seen, as the volumes increases, the variation of the crystallite size is inversely with to the main strain (see Table 1), which is can be explained by the variation of the FWHM.

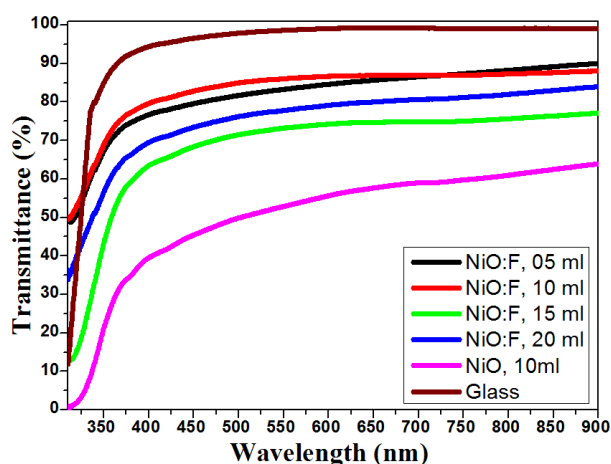


**Figure 4.** The results of the transmission spectra's of undoped and F doped NiO thin films at different NiO:F volumes.

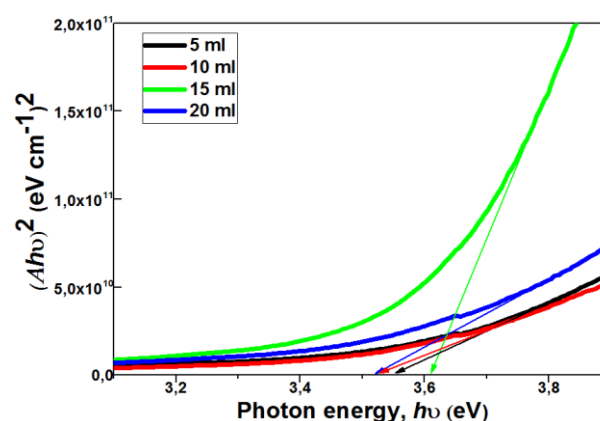


**Figure 5a.** The typical variation of values  $(Ah\nu)^2$  as a function of photon energy  $h\nu$  of F doped NiO thin films deposited at different NiO:F volumes, used to determine the optical band gap energy.

**Table 1** Shows the crystal structure of F doped NiO thin films representing of the diffraction angle, FWHM, the crystallite sizes, the lattice parameter  $a$  and main strain of the (111) plane of undoped and F doped NiO thin films as a function of NiO:F volume.

Samples	Diffraction angle $2\theta$ ( $^\circ$ )	FWHM $\beta$ ( $^\circ$ )	Crystallite size $D$ (nm)	Lattice parameter $a$ (nm)	Main strain $\mathcal{E}$
NiO, 10 ml	37,37	0,54	18,51	0,44144	0,00308
NiO:F, 05 ml	37,21	0,80	12,47	0,442662	0,00459
NiO:F, 10 ml	37,09	0,91	10,94	0,44205	0,00525
NiO:F, 15 ml	37,15	0,69	14,45	0,44032	0,00397
NiO:F, 20 ml	37,32	0,52	19,21	0,43982	0,00298

**Table 2** Shows the average transmittance and Film thickness of undoped and F doped NiO thin films as a function of NiO:F volume.

Samples	NiO, 10 ml	NiO:F, 05 ml	NiO:F, 10 ml	NiO:F, 15 ml	NiO:F, 20 ml	Glass
Average Transmittance (%) 400-800 nm	53.6	83.9	85.6	73.8	78.0	98
Film thickness (nm)	160	110	112	134	140	/

Where, the maximum crystallite size is 19.21 nm obtained for 20 ml, this is can be explained by the homogeneous in the surface and coalescence, which it's corresponded in the minimum value of lain strain (see table 1). However, the undoped NiO thin film has a main strain of 0.00308 and a crystallite size of 18.51 nm.

The optical properties of undoped and F doped NiO thin films were represented by the transmission spectra in the range of 300 to 900 nm of wavelength. Figure 4 shows the variation of the transmission of the deposited thin films at different NiO and NiO:F volumes. As the NiO:F volume increased, the transmission was decreased due to the increase in the film thickness. However, the prepared F doped NiO thin films have a good transmission is about 80 % in the visible region due to the fluorine doping (see table 2). The transmittance of 20 ml (78%) high then the 15 ml (73.8%) due to the crystallinity of the film .The region exist between 300 and 400 nm, it is the region of strong absorption, heir the transmission of F doped NiO decreased due to the excitation and the migration of the electrons from the conduction band to the valence band.

The optical band gap energy of the thin films of undoped and F doped NiO was calculated from transmission spectra, which it was applied the following equations [18-20].

$$A = \alpha d = -\ln T, \quad (4)$$

$$(Ah\nu)^2 = B(h\nu - E_g), \quad (5)$$

where  $E_g$  the optical band gap energy;  $A$  is the absorbance,  $d$  is the film thickness;  $T$  is the transmission spectra of thin films;  $\alpha$  is the absorption coefficient values;  $B$  is a constant and  $h\nu$  is the photon energy. It was found by the extrapolating the curve of  $(Ah\nu)^2$  vs  $h\nu$  at  $A = 0$  [21], which the variation was indicated in figure 5a, show the drawn of the  $(Ah\nu)^2$  as a function of  $h\nu$  of F doped NiO thin films. However, the Urbach energy of F doped NiO thin films has been determined by the following expression [21,22]:

$$A = A_0 \exp\left(\frac{h\nu}{E_u}\right), \quad (6)$$

where  $A_0$  is a constant and  $E_u$  is the Urbach energy, Figure 5b shows the variation of the drawn of  $\ln A$  as a function of the photon energy  $h\nu$ , where the Urbach energy was deduced by the inverse of the slope of the curve.

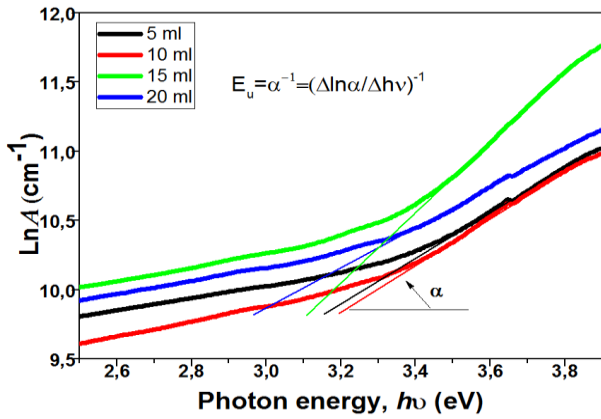


**Figure 5b.** The typical variation of values  $LnA$  as a function of photon energy  $h\nu$  of F doped NiO thin films deposited at different NiO:F volumes, used to determine the Urbach energy.

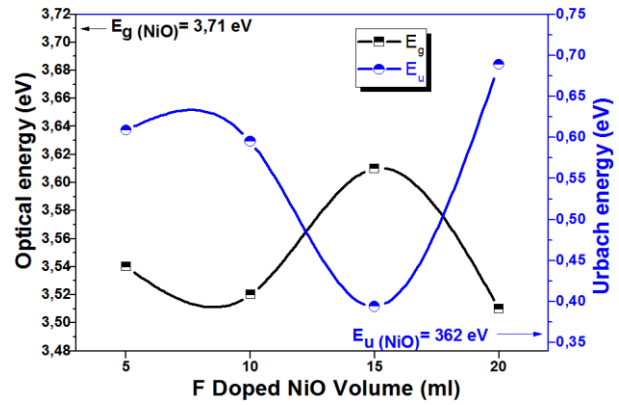


**Figure 6.** The results of optical band gap  $E_g$  and Urbach energy  $E_u$  of F doped NiO thin films at different NiO:F volumes.

**Table 3.** Shows the optical properties such as the variation of optical band gap energy and Urbach energy of undoped and F doped NiO thin films as a function of NiO:F volume.

Samples	Optical gap energy $E_g$ (eV)	Urbach energy $E_u$ (eV)
NiO, 10 ml	3.71	0.362
NiO:F, 05 ml	3,54	0,609
NiO:F, 10 ml	3,52	0,595
NiO:F, 15 ml	3.61	0,394
NiO:F, 20 ml	3,51	0,689

**Table 4.** Shows the electrical characterisations such as the variation of measured current and voltage and the sheet resistance of F doped NiO thin films as a function of the NiO:F volume.

Samples	Measured Current $I$ (nA)	Measured voltage $V$ (mV)	Sheet resistance $R_{sh}$ ( $\Omega$ )	Electrical resistivity $\rho$ ( $\Omega$ .cm)
NiO, 10 ml	0.011	5	$1.1 \times 10^{10}$	$1.5 \times 10^5 \Omega$ .cm
NiO:F, 05 ml	0,008		$2.1 \times 10^7$	231 $\Omega$ .cm
NiO:F, 10 ml	0,007		$1.7 \times 10^9$	$1.9 \times 10^3 \Omega$ .cm
NiO:F, 15 ml	0,008		$2.8 \times 10^9$	$3.8 \times 10^3 \Omega$ .cm
NiO:F, 20 ml	0,007		$2.6 \times 10^9$	$3.6 \times 10^3 \Omega$ .cm

**Table 5.** The comparative study of the structural, optical and electrical properties of undoped and F doped NiO thin films.

Thin films	Experiments	Film thickness (nm)	Crystallite size $G$ (nm)	Transmittance (%)	Optical Band Gap $E_g$ (eV)	Sheet resistance or electrical resistivity	Ref.
NiO NiO: 1F% NiO: 5F% NiO: 10F%	- Spray deposition - ST=400 °C - 0.1M - 0.3 mL/s		25 35 21.9 13.5	75 75+1 75+2 75+2	3.67 3.72 3.71 3.72	18 $\Omega$ cm 2 $\Omega$ cm 14 $\Omega$ cm 18 $\Omega$ cm	[23]
NiO NiO: 1Li% NiO: 2Li% NiO: 3Li% NiO: 4Li% NiO: 5Li%	- Spray deposition - ST= 500 °C - 0.1M - 13 mL	197 236 221 374 435 421	41 59 31 45 44 36	59 32 48 37 50 47	3.865 3.744 3.697 3.738 3.714 3.716	- $2.403 \times 10^9 \Omega$ $1.195 \times 10^7 \Omega$ $7.984 \times 10^6 \Omega$ $1.386 \times 10^7 \Omega$ $1.694 \times 10^7 \Omega$	[24]
NiO NiO: 1Cu% NiO: 2Cu% NiO: 3Cu% NiO: 4Cu% NiO: 5Cu%	- Spray deposition - ST= 410 °C - 0.2 M		64 37 51 38 51 57	about 50	3.572 3.519 3.536 3.461 3.473 3.467	2712 $\Omega$ cm 589 $\Omega$ cm 490 $\Omega$ cm 1106 $\Omega$ cm 545 $\Omega$ cm 669 $\Omega$ cm	[25]
NiO, 10ml NiO:F, 05ml NiO:F, 10ml NiO:F, 15ml NiO:F, 20ml	- Spray deposition - ST=400 °C - 0.1M - F/Ni = 4%	160 110 112 134 140	18.51 12.47 10.94 14.45 19.21	53.6 83.9 85.6 73.8 78.0	3.71 3,54 3,52 3,61 3,51	$1.5 \times 10^5 \Omega$ .cm 231 $\Omega$ .cm $1.9 \times 10^3 \Omega$ .cm $3.8 \times 10^3 \Omega$ .cm $3.6 \times 10^3 \Omega$ .cm	This Work

Figure 6 shows the variation of the band gap energy and the Urbach energy of newly deposited F doped NiO thin films at different volumes. As can be seen, as the volumes increases, the variation of the optical energy is inversely with the Urbach energy (see table 3). The film deposited with 20 ml has a minimum optical energy and maximum Urbach energy, this is can be explained by the increased movement of F in the NiO:F, and the corporation between F and O and thus there is an increase in the substitutional site. However, the undoped NiO thin film has a highest the optical energy of 3.71 eV and a minimum the Urbach energy of 0.362 eV (see Table 3).

The electrical conductivity of F doped NiO thin films was determined by four- point probe technique, it is based on the measured voltage, current and sheet resistance expressed by:

$$R_{sh} = \frac{1}{d} \left( \frac{\pi}{\ln 2} * \frac{V}{I} \right), \quad (7)$$

$$\sigma = \frac{1}{\rho} = \frac{1}{dR_{sh}}, \quad (8)$$

where  $R_{sh}$  is the electrical resistivity;  $d$  is the film thickness;  $\sigma$  is the conductivity;  $\rho$  is the resistivity;  $V$  is the applied voltage =5V and  $I$  is the measurement current (see Table 4). As can be seen, as the volume increases, the electrical resistivity increases from 5 to 15 ml (see table 4), this increase can be explained by the decrease in the number of electrons and mobility, leading to a p-type semiconductor. However, the undoped NiO

thin film has a highest electrical resistivity of  $1.5 \times 10^5 \Omega \cdot \text{cm}$  and the F doped NiO thin film with 5 ml has a minimum the electrical resistivity of 231  $\Omega \cdot \text{cm}$  (see Table 3).

The comparative study of the structural, optical and electrical properties of undoped and F doped NiO thin films are presented in Table 5, as can be seen, we have a lowest crystallite size, good transmittance and good electrical property.

#### 4. Conclusion

In the conclusion, the structural, optical and electrical properties of undoped F doped NiO thin films were investigated. The thin films of F doped NiO were deposited by spray technique at substrate temperature of 450 °C with different NiO:F solution volumes of 5, 10, 15 and 20 ml. The prepared F doped NiO thin films have a monocrystalline nature with a cubic structure, the (111) diffraction peak is the preferred orientation, the maximum crystallite size is 19.21 nm obtained for 20 ml. The optical property shows that the all the prepared F doped NiO thin films have a good transmittance which is about 80 % in the visible region. The F doped NiO thin films deposited with 20 ml have minimum optical gap energy of 3.51 eV and the highest value of Urbach energy is 0,689 meV. However, the thin film prepared with 5 ml has a minimum electrical resistivity of 231  $\Omega \cdot \text{cm}$ , which can be used as a gas sensing.

#### References

1. M H Raza, K Movlaee, Y Wu, S M El-Refaei, M Karg, S G Leonardi, G Neri, and N Pinna, *Chem. Electro. Chem* **6** (2019) 383.
2. S H Wang, S R Jian, G J Chen, H Z Cheng, J Y Juang, *Coatings* **9** (2019) 107.
3. Y Aoun, M Marrakchi, S Benramache, B Benhaoua, S Lakel, and A Cheraf, *Materials Research* **21** (2018) e20170681.
4. C Zauouche, A Gahtar, S Benramache *et al. Digest Journal of Nanomaterials & Biostructures (DJNB)* **17** (2022) 1453
5. R S Kate, S C Bulakhe, and R J Deokate, *Journal of Electronic Materials* **48** (2019) 3220.
6. V Panneerselvam, K K Chinnakutti, S T Salammal, A K Soman, K Parasuraman, V Vishwakarma, and V Kanagasabai, *Applied Nanoscience* **8** (2018) 1299.
7. M Z Muzamil Aftab, A Dilawar, F Bashir, and Z H Aftab, *Ceramics International* **46** (2020) 5037.
8. M Sh Abdel-wahab, H K El Emam and W M A El Roubi, *RSC Advances* **13** (2023) 10818.
9. K Sato, S Kim, S Komuro and X Zhao, *Japanese Journal of Applied Physics* **55** (2016) 06GJ10.
10. N R Aswathy, J J Varghese, Sh Ranjini Nair, and R Vinod Kumar, *Materials Chemistry and Physics* **282** (2022) 125916.
11. H S Rasheed, H I Abdulgafour, F M Hassan *et al. Journal of Materials Science: Materials in Electronics* **33** (2022) 18187.
12. I L P Raj, S Valanarasu, A Asuntha *et al. Journal of Materials Science: Materials in Electronics* **33** (2022) 11753.
13. X Chu, J Leng, J Liu *et al. Journal of Materials Science: Materials in Electronics* **27** (2016) 6408.
14. M S Abdel-wahab, H K El Emam. & W M A El Roubi, *Journal of Materials Science: Materials in Electronics* **34** (2023) 1637.
15. Y Zhao, J Yan, Y Huang *et al. Journal of Materials Science: Materials in Electronics* **29** (2018) 11498.
16. R S Kate, S C Bulakhe and R J Deokate, *Opt. Quant. Electron.* **51** (2019) 319.
17. H H Abdelhalium, M S Abdel-wahab, M T Tamm and W Z Tawfik, *Appl. Phys. A*, **129** (2023) 459.
18. A Diha, S Benramache and L Fellah, *J. Nano- Electron. Phys.* **11** (2019) 03002.
19. A Kumar and P P Sahay, *Appl. Phys. A*, **127** (2021) 286.
20. A Gahtar, S Benramache, A Ammari, A Boukhachem and A Ziouche, *Inorg. Nano-Metal Chem.* **52** (2022) 112.
21. U Alver, H Yaykaşlı, S Kerli and A Tanrıverdi, *Int. J. Min. Met. Mater.* **20** (2013) 1097.
22. H Aydin, Sh A. Mansour, C Aydin, A A Al-Ghamdi, O A. Al-Hartomy, F El-Tantawy and F Yakuphanoglu, *J. Sol-Gel Sci. Techn.* **64** (2012) 728.

23. S Kerli, and U Alver, *Crystallogr. Rep.* **59** (2014) 1103.
24. D P Joseph, M Saravanan, B Muthuraaman, P Renugambal, S Sambasivam, S P Raja, P Maruthamuthu and C Venkateswaran, *Nanotechnology* **19** (2008) 485707.
25. M Aftab, M Z Butt, D Ali, F Bashir and T M Khan, *Opt. Mater.* **119** (2021) 111369.